Journal of Petroleum Science and Engineering 170 (2018) 62–70

Contents lists available at ScienceDirect

Journal of Petroleum Science and Engineering

journal homepage: www.elsevier.com/locate/petrol

Numerical simulation of reaction under high pressure conditions for thermal spallation drilling

Zehao Lyu, Xianzhi Song*, Gensheng Li

State Key Laboratory of Petroleum Resources and Prospecting, China University of Petroleum, Beijing, Beijing, 102249, China

ARTICLE INFO

Keywords:
Thermal spallation
Reaction
Numerical simulation
High pressure

ABSTRACT

Thermal spallation technology is a drilling method, which is potentially suitable for the exploitation of petroleum in hard rocks with low costs. In this paper, characteristics of reaction are investigated under relatively high pressure in thermal spallation drilling. The Peng-Robinson equation of state and eddy dissipation model are applied in the simulation. Effects of methane and oxygen flow rate, nitrogen fraction on the flow field are studied. Simulation results are validated in experiments that monitor the temperature of the flame jet using thermocouples. Results show that besides a portion of oxygen reacting with the methane, the left oxygen mainly flows towards the boundary of the reactor. The reaction between methane and oxygen mainly occurs at the central part of the reactor. Also, the temperature close to the wall of the reactor is only 1300 K, which can help to protect the reactor wall from damage due to high temperature. Increasing the methane flow rate within a certain range can help to obtain high temperature and high jet velocity simultaneously. Also, injecting mixture of oxygen and nitrogen can prevent too much excessive oxygen from existing in the wellbore during thermal spallation drilling. Results in this paper could provide guidance for field applications.

1. Introduction

During the drilling process, the hardness of rock in deep formation is high and the drill-ability is poor. For traditional rotary drilling methods, the loss of drilling mechanical energy and hydraulic energy is large along the drill string. Besides, the contact between the drill bit and rock, continual tripping and making connections has led to the abrasion of drill bit and thus is time-consuming and has high drilling costs (Rauenzahn and Tester, 1985). Therefore, it is necessary to develop some alternative efficient drilling methods for drilling in deep formations.

Thermal spallation drilling technology uses high temperature flame or fluid to produce non-uniform expansion stresses within the rock (Calaman and Rolseth, 1968; Browning et al., 1965). The fuel and oxidizer are usually injected to the downhole reactor through the coiled tubing, where the fuel and oxidizer are ignited to generate high temperature reaction products (Fig. 1). Due to stresses, thermally-induced fragmentation occurs and disk-like rock fragments are formed in the heated rock's spallation zone (Heard, 1980; Li et al., 2014). The entire thermal spallation process can be divided into three stages: the initiation stage, the expansion stage and the stripping stage (Fig. 1) (Yan et al., 1999; Tan et al., 2006; Wu and Liu, 2003). Since contact is avoided between the reactor and the rock surface, a longer life is obtained for the drilling tool, when compared to traditional rotary drilling equipment, due to less wear (Tester et al., 1994). In relatively deep formations, the high velocity of the flame jet is required to provide sufficient energy to carry the drilling cuttings upward to the surface via the annulus (Browning et al., 1965).

Thermal spallation drilling was commercially developed for drilling blast holes in the mining industry starting in 1947 by the Linde Air Division of Union Carbide. These systems used a flame jet-piercing tool to drill blast holes for mining ore. By 1961, the tool had been used in the production of 140 million tons of crude taconite ore, as well as 25 million tons of granite, quartzite, syenite and sandstone (Calaman and Rolseth, 1962; Augustine and Potter, 2007). Researches about thermal spallation drilling mainly focus on experimental study on the characteristics of rock under high temperature and high pressure conditions and numerical simulation on the initiated micro-cracks in the rock. Early work by Rauenzahn (1986) and Tester (1990) established the basis for this study and focused on characterization of fundamental mechanisms of spall formation and ejection and on modeling fluid flow and heat transfer process important to simulating drilling and quarrying conditions observed in practice. Besides, several analytical models have been developed based on buckling theory (Thirumalai, 1969). Researchers also employed Weibull statistical failure theory to represent the relationship between microstructural heterogeneity and the rock's

* Corresponding author.
E-mail address: songxz@cup.edu.cn (X. Song).

https://doi.org/10.1016/j.petrol.2018.06.049
Received 13 October 2017; Received in revised form 13 June 2018; Accepted 18 June 2018
Available online 19 June 2018
0920-4105/

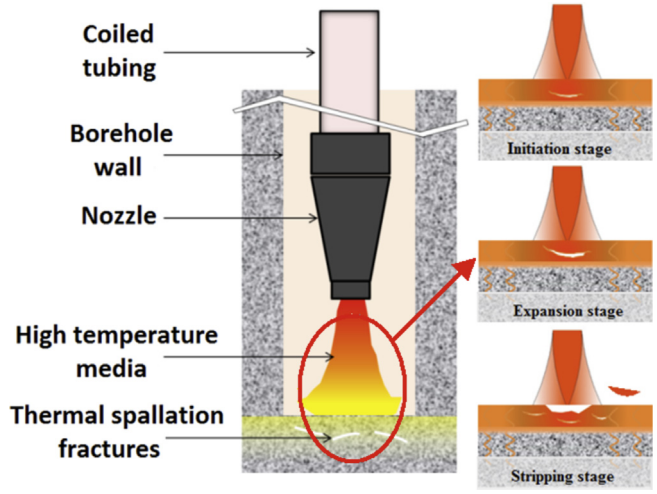

Fig. 1. Bottomhole assembly in thermal spallation drilling and thermal spallation process.

propensity to spall (Weibull, 1950; Dey and Kranz, 1985; Rauenzahn and Tester, 1991). Walsh and Lomov, 2013 described a numerical modeling tool designed to conduct explicit simulations of thermal spallation at the grain-scale. The model used an Eulerian-Godunov scheme to simulate solid and fluid mechanical behavior. Besides, Lyu et al. (2017) tried to optimize the combustion model to simulate the thermal jet more accurately with less computational costs. Specific energy analysis and investigations on the micro-structure of rock were also performed (Lyu et al., 2018a, 2018b).

However, to the best of our knowledge, the study on the generation of flame jet is scarce. Besides, previous investigations on thermal spallation drilling are under the conditions of lower than 10 MPa. If the thermal spallation technique is used at depths larger than 1 km, the carrying capacity of cuttings has to be studied. What is more important is that the generated carbon dioxide reaches a supercritical state at pressure larger than 10 MPa. The drilling using pure supercritical carbon dioxide is also a relatively novel method, which has been proposed and widely reported in the literature (Wang et al., 2011; Yu-Kun et al., 2013; Ni et al., 2016). The rock-breaking ability tests carried out by Kolle (2000) indicated that supercritical carbon dioxide jet had improved rock-breaking efficiency. The threshold pressure was 2/3 that of water jet for granite and less than half that of water jet for shale. Therefore, the thermal spallation applied in relatively deep formations (> 1 km) can be promising because of the coupled effects of supercritical carbon dioxide impact and high temperature.

The presented work is aimed to develop a numerical model for the simulation of the generation of thermal jet under relatively high pressure. Characteristics of reaction flow field are investigated. The Peng-Robinson equation of state and Eddy Dissipation Model (EDM) are applied in the simulation. Effects of methane and oxygen flow rate, nitrogen fraction on the flow field are studied. An experimental setup is designed and experiments are conducted to verify the simulation results.

2. Model development

2.1. Geometry description

Simulations are carried out by using the established geometric model as shown in Fig. 2. To simplify the numerical simulation of this axisymmetric circular downhole reactor, a two-dimensional model is used to represent the real three-dimensional situation. The fuel (methane) and oxidizer (oxygen) are injected to the downhole reactor through separate conduits. In the reactor, the injected methane and

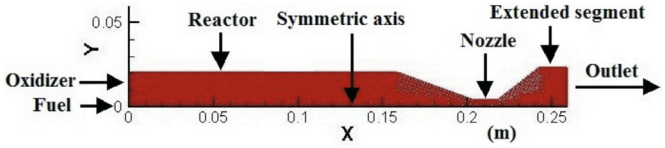

Fig. 2. Geometric model of the reaction chamber.

Table 1
Specific dimensions of the reaction chamber.

Reaction chamber length (mm)	Reaction chamber diameter (mm)	Fuel inlet diameter (mm)	Oxygen inlet diameter (mm)	Nozzle diameter (mm)
259	40/46	3.0	4.0	8.0

oxygen are mixed. Then a nozzle is applied to enhance the generated flame jet. An extended segment is also used to concentrate the jet discharged from the nozzle. The specific dimensions of the reactor are displayed in Table 1. The total number of grids is 12326 and other grids are checked for grid independence and produce similar results.

2.2. Simulation model

The conservation equations for momentum, mass and energy are solved in conjunction with a suitable turbulence model. All quantities are time-averaged quantities arising from Reynolds averaging of the instantaneous equations (Song et al., 2017a,b):

$$\frac{\partial \rho}{\partial t} + \frac{\partial \rho u_j}{\partial x_j} = 0 \tag{1}$$

$$\frac{\partial \rho u_i}{\partial t} + \frac{\partial \rho u_i u_j}{\partial x_j} = -\frac{\partial p}{\partial x_i} + \frac{\partial \tau_{ij}}{\partial x_j} + S_m \tag{2}$$

Eqs. (1) and (2) represent the mass and momentum equations. ρ is the density. u_i is the velocity. p is the pressure. τ_{ij} is the viscous stress. S_m is the source term including gravity. t is the time.

The transport equation for the total specific energy (e) in Fluent is (Song et al., 2017a,b):

$$\frac{\partial(\rho e)}{\partial t} + \frac{\partial[u_i(\rho e + p)]}{\partial x_j} = \frac{\partial}{\partial x_i}\left[\lambda_{eff}\frac{\partial T}{x_j} + u_i(\tau_{ij})_{eff}\right] \tag{3}$$

where λ_{eff} is the effective thermal conductivity. $(\tau_{ij})_{eff}$ is the deviatoric stress tensor.

With respect to the standard $k-\varepsilon$, the turbulence kinetic energy k, and its rate of dissipation ε, are obtained from the following transport equations:

$$\frac{\partial}{\partial t}(\rho k) + \frac{\partial}{\partial x_i}(\rho k u_i) = \frac{\partial}{\partial x_j}\left[\left(\mu + \frac{\mu_t}{\sigma_k}\right)\frac{\partial k}{\partial x_j}\right] + G_k + G_b\rho\varepsilon - Y_M + S_k \tag{4}$$

$$\frac{\partial}{\partial t}(\rho \varepsilon) + \frac{\partial}{\partial x_i}(\rho \varepsilon u_i) = \frac{\partial}{\partial x_j}\left[\left(\mu + \frac{\mu_t}{\sigma_\varepsilon}\right)\frac{\partial \varepsilon}{\partial x_j}\right] + C_{1\varepsilon}\frac{\varepsilon}{k}(G_k + C_{3\varepsilon}G_b) - C_{2\varepsilon}\rho\frac{\varepsilon^2}{k} + S_\varepsilon \tag{5}$$

where μ is the molecular viscosity and μ_t is the turbulent viscosity. σ_k and σ_ε are turbulent Prandtl numbers. G_k is the turbulence kinetic energy due to the mean velocity gradients and G_b represents the turbulence kinetic energy due to buoyancy. Y_M is the contribution of the fluctuating dilatation and S_k and S_ε are user-defined source terms. $C_{1\varepsilon}$, $C_{2\varepsilon}$ and $C_{3\varepsilon}$ are constants.

In addition to the continuity equation, the momentum equation, the energy equation and the standard $k-\varepsilon$ turbulence model are also considered. The reaction products include water and carbon dioxide. In